JOURNAL OF VIROLOGY, Dec. 1997, p. 9701–9712 Vol. 71, No. 12
0022-538X/97/$04.00+0

Role of Sialyloligosaccharide Binding in Theiler's Virus Persistence

LAN ZHOU,[1,2] XIAOXU LIN,[1] TODD J. GREEN,[1,2] HOWARD L. LIPTON,[3,4] AND MING LUO[1,2]*

Department of Microbiology[1] and Center for Macromolecular Crystallography,[2] University of Alabama at Birmingham, Birmingham, Alabama 35294; Division of Neurology, Evanston Hospital, Evanston, Illinois 60201[3]; and Department of Biochemistry, Molecular Biology and Cell Biology, Northwestern University, Evanston, Illinois 60208[4]

Received 31 March 1997/Accepted 28 August 1997

Theiler's murine encephalomyelitis viruses (TMEVs) belong to the *Picornaviridae* family and are divided into two groups, typified by strain GDVII virus and members of the TO (Theiler's original) group. The highly virulent GDVII group causes acute encephalitis in mice, while the TO group is less virulent and causes a chronic demyelinating disease which is associated with viral persistence in mice. This persistent central nervous system infection with demyelination resembles multiple sclerosis (MS) in humans and has thus become an important model for studying MS. It has been shown that some of the determinants associated with viral persistence are located on the capsid proteins of the TO group. Structural comparisons of two persistent strains (BeAn and DA) and a highly virulent strain (GDVII) showed that the most significant structural variations between these two groups of viruses are located on the sites that may influence virus binding to cellular receptors. Most animal viruses attach to specific cellular receptors that, in part, determine host range and tissue tropism. In this study, atomic models of TMEV chimeras were built with the known structures of GDVII, BeAn, and DA viruses. Comparisons among the known GDVII, BeAn, and DA structures as well as the predicted models for the TMEV chimeras suggested that a gap on the capsid surface next to the putative receptor binding site, composed of residues from VP1 and VP2, may be important in determining viral persistence by influencing virus attachment to cellular receptors, such as sialyloligosaccharides. Our results showed that sialyllactose, the first three sugar molecules of common oligosaccharides on the surface of mammalian cells, inhibits virus binding to the host cell and infection with the persistent BeAn virus but not the nonpersistent GDVII and chimera 39 viruses.

Theiler's murine encephalomyelitis viruses (TMEVs) belong to the *Picornaviridae* family and are cardioviruses, based on sequence analysis (26–28). TMEVs were first discovered in laboratory mice suffering from hind-leg paralysis (34). The TMEVs are divided into two groups based on neurovirulence. One group consists of strains that cause rapid destruction of neurons. These viruses infect and kill their hosts from severe encephalitis in a matter of days. GDVII and FA belong to this group of TMEVs and are defined as neurovirulent strains. The other group of TMEVs is the TO (Theiler's original) group, comprised of strains that cause a persistent central nervous system (CNS) infection and inflammatory demyelination (18). Contained in this group are strains DA, BeAn, TO4, WW, and Yale. Infection of mice with a persistent strain results in a biphasic disease of the CNS. In the first phase of the disease, there is a mild encephalitis characterized by the replication of virus in neurons of the brain. This is followed by a second phase in which the virus migrates to the spinal cord, first to the gray and then to the white matter, where it persists, and a chronic, inflammatory demyelination closely resembling multiple sclerosis can be observed (8, 18). For this reason, TMEVs are useful as an animal model for the study of multiple sclerosis, a chronic disease in humans.

Atomic structures of TMEVs from each group have been determined by X-ray crystallography. Structures for strains BeAn, DA, and GDVII have been reported (13, 21, 22). There is over 90% sequence identity between GDVII and BeAn or between GDVII and DA (see Fig. 2). Like those of all other picornaviruses, each of the 60 icosahedral protomers in TMEVs contains four viral polypeptides: VP1, VP2, VP3, and VP4. Only VP1, VP2, and VP3 are exposed on the surface of the virus and make up its outer protein shell. VP1, VP2, and VP3, with molecular masses of 37, 34, and 25 kDa, respectively, contain a common eight-stranded, antiparallel, β-barrel folding motif (13, 21, 22). Their amino termini intertwine to form a network on the interior of the protein shell. Five VP3 amino termini come together to form a five-stranded helical β-cylinder in the virion interior around each icosahedral fivefold axis. This β-cylinder stabilizes the pentamer and is thought to be important for its assembly in other picornaviruses (3, 14, 29), and it may have the same function in TMEVs.

Chimeric viruses involving the exchange of genomic nucleotide sequences corresponding to the capsid regions of neurovirulent and persistent strains of TMEVs have been constructed in order to assess regions of the capsid that affect persistence and neurovirulence. In general, data from studies by different laboratories consistently showed that the viral capsid bears the main determinants of viral persistence and neurovirulence. When the capsid in a neurovirulent strain GDVII background was replaced with the persistent strain BeAn or DA fragment, the resulting chimeric viruses displayed persistence in the CNS and complete attenuation of the high degree of neurovirulence (2, 6, 11, 23). Conversely, replacing the capsid of BeAn or DA with that of GDVII could yield a persistent or nonpersistent chimeric virus, depending on the length of the replacing fragment (2). In addition, mutations at residue 1101 in VP1 and 2141 in VP2 were shown to influence the persistence of strain DA (15, 39). In this study, homology modeling was carried out for 12 TMEV chimeras by use of the crystallographic coordinates of the previously reported virus structures (GDVII, DA, and BeAn) and the homology modeling program MODELLER (32). By comparison of persistent na-

* Corresponding author. Phone: (205) 934-4259. Fax: (205) 934-0480. E-mail: ming@orion.cmc.uab.edu.

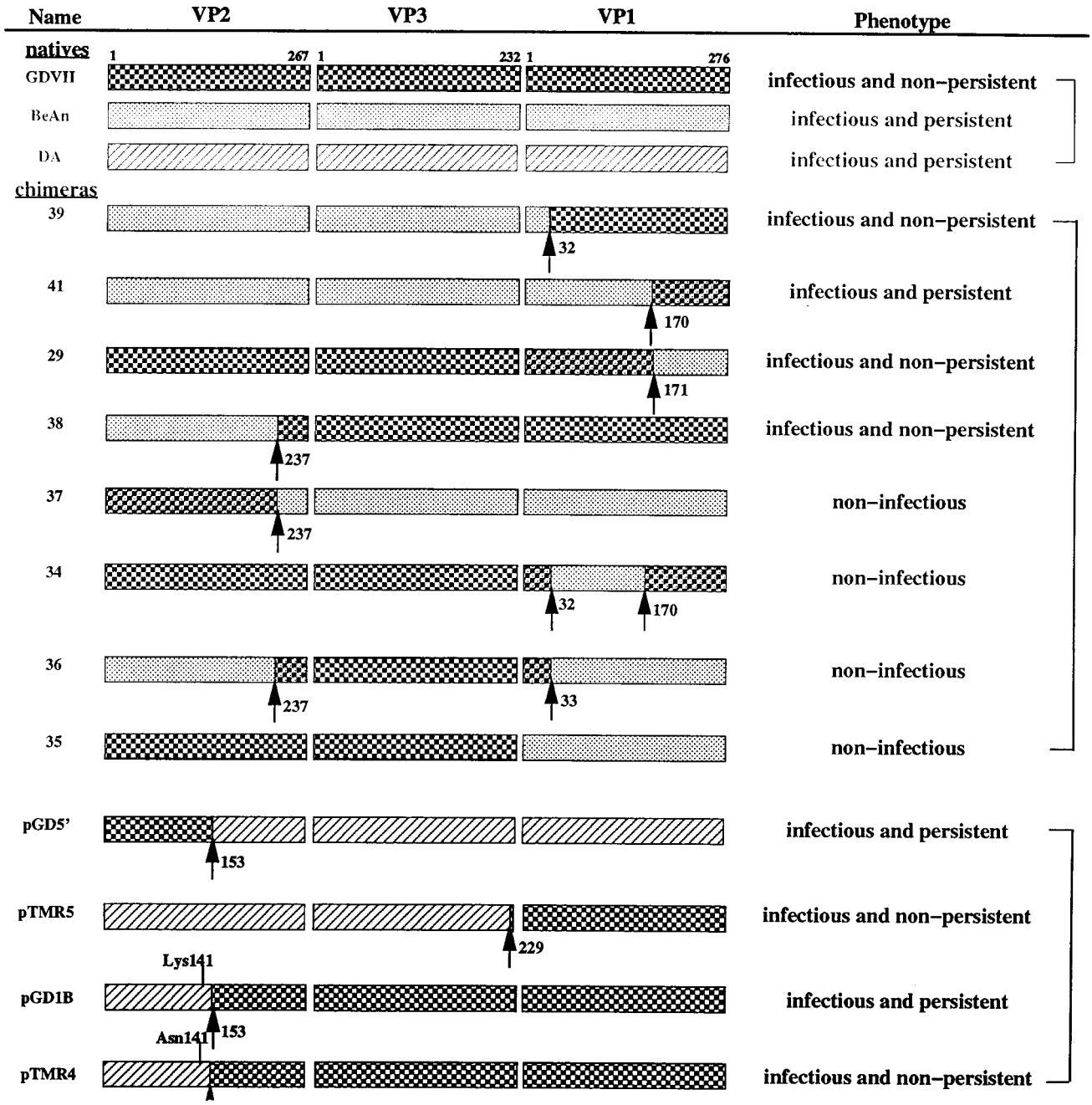

FIG. 1. Capsid protein constructs of TMEV chimeras and the corresponding phenotypes. Data for native viruses were from Lipton (18). Data for chimeras were from Adami et al. (2). Data for pGD5′, pTMR5, pGD1B, and pTMR4 were from Jarousse et al. (15).

tive and chimeric structures with neurovirulent native and chimeric structures, we looked for insights into the molecular differences that might be responsible for TMEV persistence. One of the potential determinants that we identified is a gap between VP1 and VP2 on the viral surface. We postulate that this gap is related to binding by the persistent TMEVs to part of the host receptor, sialyloligosaccharides, but not by the nonpersistent TMEVs. This idea is supported by the findings in this study that only the binding of and infection with persistent BeAn virus, and not nonpersistent GDVII and chimera 39 viruses, were inhibited by sialyllactose, the terminal three sugar molecules of oligosaccharides on the cell surface.

MATERIALS AND METHODS

Coordinates and sequences of TMEVs. The structures of BeAn and GDVII viruses were determined in our laboratory (21, 22). Atomic coordinates of DA virus were obtained from the Brookhaven Protein Data Bank (13). Amino acid sequences for the TMEV chimeras were deduced based on DNA constructions (Fig. 1).

Modeling of TMEV chimeras. Structural models for each of the chimeras were built by use of the homology modeling program MODELLER (32). MODELLER uses experimentally determined protein structures to predict the conformation of other proteins with similar amino acid sequences by satisfaction of spatial restraints. MODELLER automatically derives the restraints from the known homologous structures and their alignment with the target sequence. The three-dimensional structure of the target is first predicted by optimization of a molecular probability density function. The molecular probability density func-

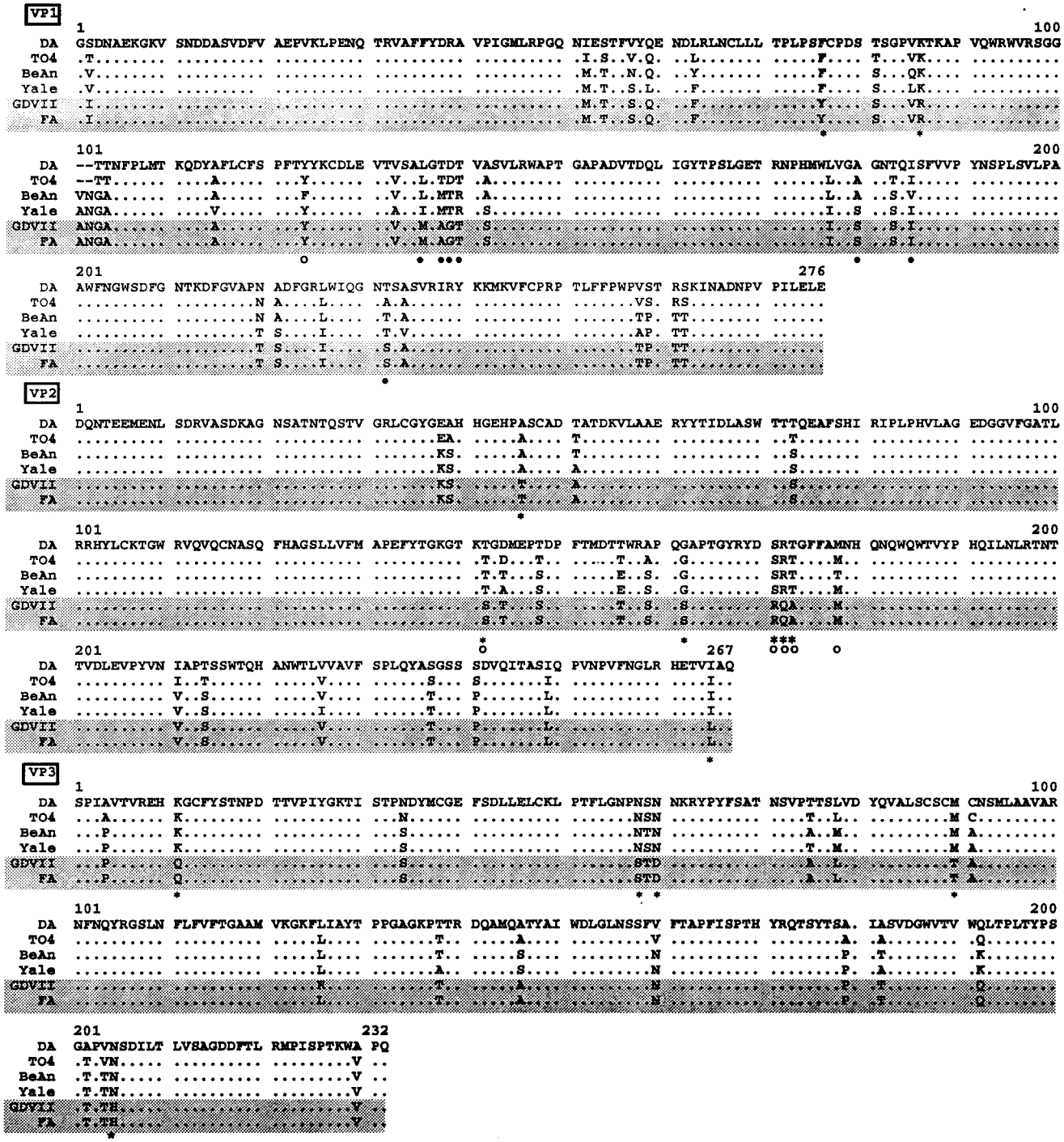

FIG. 2. Sequence alignment of TMEV capsid proteins VP1, VP2, and VP3. Sequences of DA, BeAn, and GDVII were obtained from GenBank, and sequences of TO4, Yale, and FA were obtained from Michiels et al. (24). Sequences for nonpersistent native viruses GDVII and FA are shaded in gray. Asterisks indicate the amino acids which are conserved in the persistent group but which are different from those in the nonpersistent group. Variable residues are indicated by filled circles in cluster A and by empty circles in cluster B.

tion is then optimized with a variable-target-function procedure in Cartesian space that utilizes methods of conjugate gradient and molecular dynamics with simulated annealing (31). Briefly, the hybrid subunit (e.g., VP1) of each TMEV chimera was built by use of its counterpart from the known TMEV structures based on the sequence alignment. The hybrid subunit was optimized in the absence of the other two subunits (e.g., VP2 and VP3) in the icosahedral asymmetric unit. Then, the structure of this hybrid subunit was energetically refined in the presence of the other two subunits, with or without fixing the movement of the latter by use of X-PLOR (5).

Structural comparisons. The structural observations and comparisons were performed with FRODO (16) on an Evans and Southerland graphics workstation. The outer surface of the virus was calculated with the program ROADMAP (7), and viral surface contours were generated with the program GRASP (25).

Cells and media. BHK-21 cells (American Type Culture Collection) were grown in monolayers in Dulbecco's modified Eagle's medium (DMEM; ICN Biochemicals) supplemented with L-glutamine and penicillin-streptomycin (ICN) and 10% fetal bovine serum (Biocell Laboratories) at 37°C in 5% CO_2.

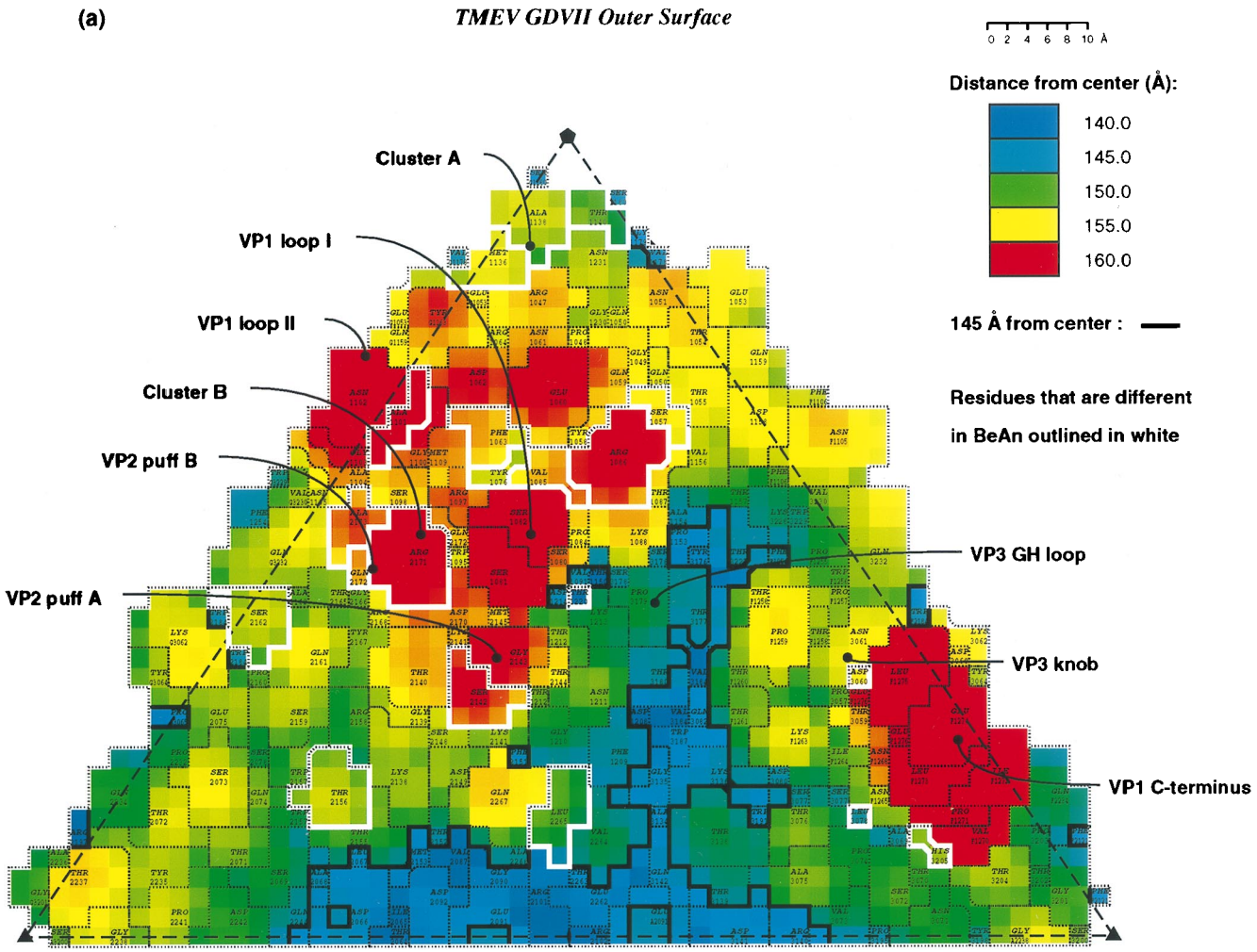

FIG. 3. (a) Two-dimensional road map of residues that shape the GDVII outer surface within one icosahedral unit. The distances from the residues to the virion center are coded in different colors. The putative receptor binding site near the VP3 GH loop is outlined as described by Rossmann and Palmenberg (30) with the program ROADMAP. Residues that are different in BeAn are outlined in white. (b) Two-dimensional road map of residues that shape the BeAn outer surface within one icosahedral unit. The distances from the residues to the virion center are coded in different colors. Residues near the gap between VP1 loops I and II and the VP2 puff are outlined in white. (c) Surface contour of one icosahedral unit of BeAn (c1). The region including the VP3 GH loop and the gap is boxed in red. The corresponding boxed regions for BeAn, DA, and GDVII are enlarged in c2, c3, and c4, respectively, with the program GRASP.

TMEVs and radiolabeling of BeAn virus. BeAn, GDVII, and chimera 39 viruses were propagated in BHK-21 cells and purified by density centrifugation by a previously described procedure (35). To radiolabel BeAn virus, BHK-21 cell monolayers were infected with BeAn virus at a multiplicity of infection of 20. After 90 min of adsorption at 37°C, cells were washed twice with serum-free DMEM and then with Met-Cys–free medium. After the infected cells were starved in the same deficient medium for 15 min at 37°C, a mixture of deficient and complete media (5:1 ratio) containing 40 μCi of [^{35}S]Met-Cys (Amersham) per ml was added, and the infection was allowed to proceed until an extensive cytopathic effect (CPE) was observed. Radiolabeled viruses were purified as described elsewhere (35).

Inhibition of TMEV infection and binding by sialyllactose in BHK-21 cells. To test the effect of sialyllactose on infections with parental TMEVs (BeAn and GDVII) and chimera 39, virus concentrations of purified BeAn, GDVII, or chimera 39 samples were equalized based on the UV absorptions at 260 and 280 nm. Virus inocula for infection were prepared by mixing equal volumes of BeAn, GDVII, or chimera 39 virus and different dilutions of sialyllactose (Boehringer Mannheim), followed by incubation for 10 min at 24°C. The BHK-21 cell monolayers were then infected with each virus inoculum. After 90 min of adsorption, the inoculum was removed, and the cells were washed twice with warmed phosphate-buffered saline (PBS) (pH 7.4) and maintained in DMEM at 37°C in 5% CO_2. Virus yields under each condition were determined by a plaque assay with six-well plates (Costar) containing confluent monolayers of BHK-21 cells as described previously (19). For direct virus binding, BHK-21 cell monolayers were grown to 90% confluence in six-well plates and then incubated for 3 h at 4°C. Cells were washed twice with PBS before the addition of ^{35}S-labeled TMEV at 1.16×10^5 cpm/well in DMEM with 0.0, 5.0, or 9.0 mM sialyllactose. The adsorption process was carried out at 4°C to minimize virus internalization into the cells. At various times, cells were washed three times with cold PBS and removed with lysis buffer containing 1% Nonidet P-40, 0.1% sodium dodecyl sulfate, and 0.5% deoxycholate. Half of each sample was used for radioactivity counting.

RESULTS AND DISCUSSION

Structural differences among native viruses. Although the phenotype of GDVII is very different from that of BeAn and DA, TMEV strains of both the highly virulent and the TO groups have very high overall sequence identities, >90% at the amino acid level (Fig. 2). The three-dimensional structural differences between GDVII and BeAn or DA viruses are small and localized. The root-mean-square deviations between the Cα coordinates of GDVII versus BeAn or GDVII versus DA are 0.71 and 0.78 Å, respectively, for each counterpart residue in VP1, VP2, and VP3. Two clusters of unconserved amino acid changes (clusters A and B) were mapped on the virus surfaces. Cluster A is near the third corner of VP1, while

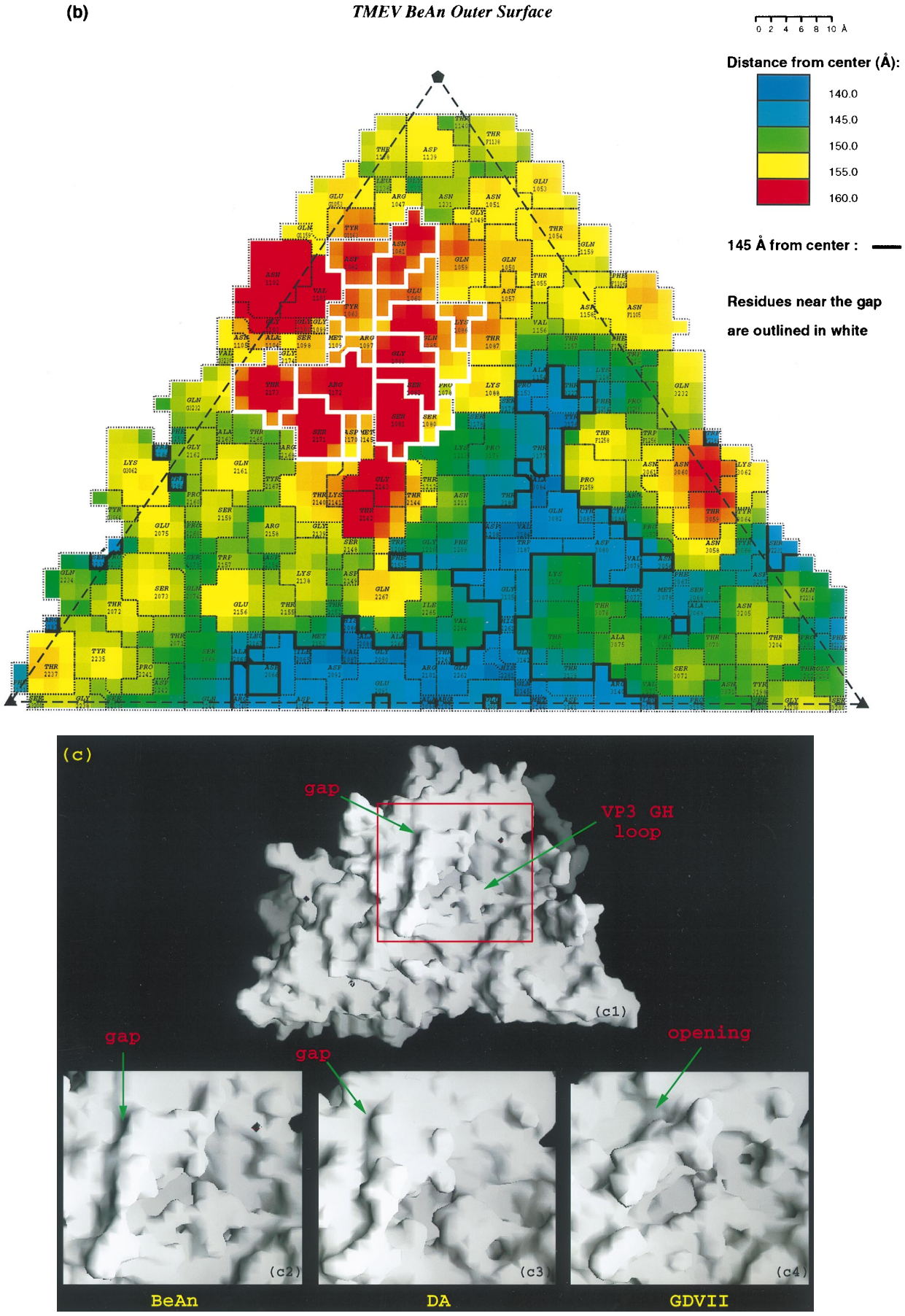

FIG. 3—*Continued.*

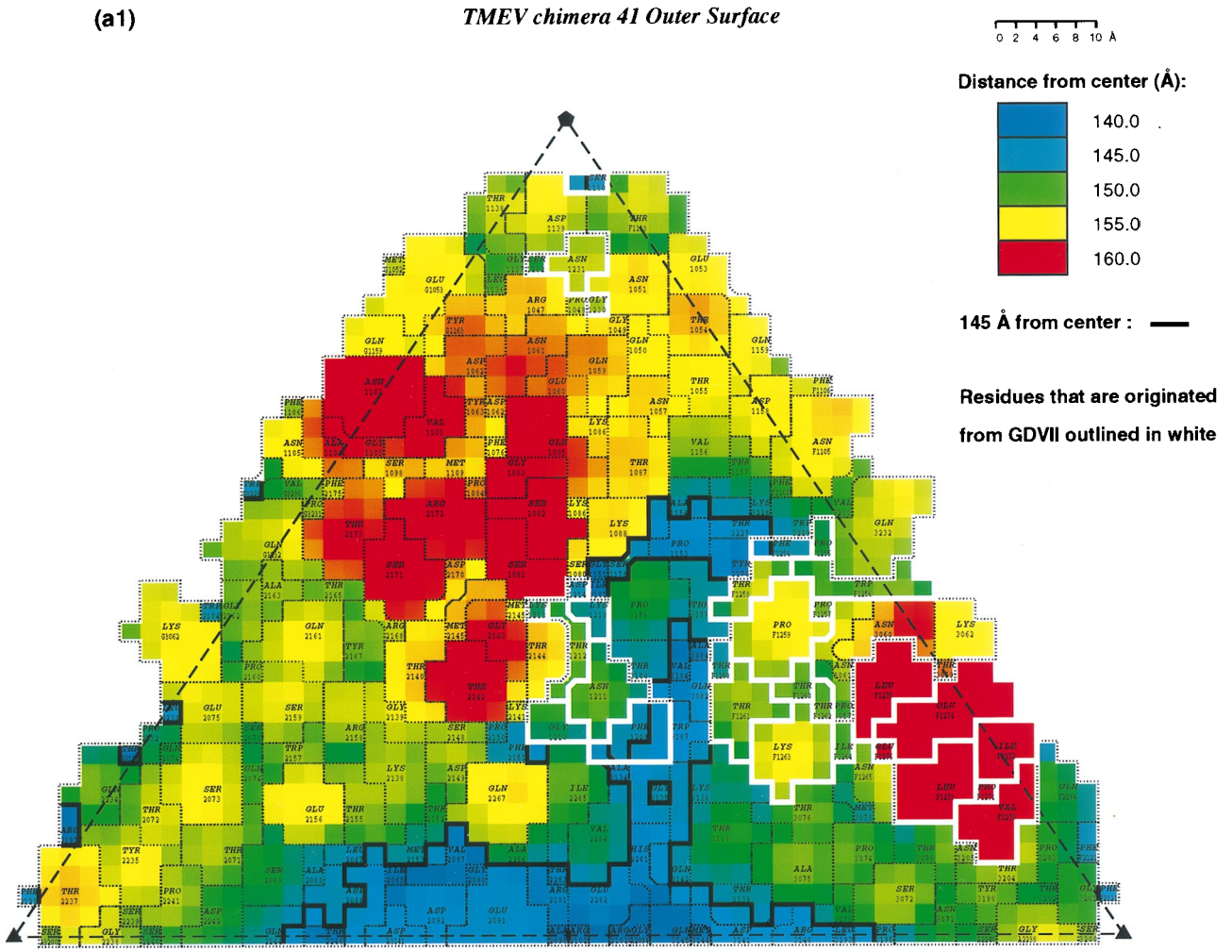

FIG. 4. (a) Two-dimensional road map of residues that compose chimera 41 (a1) and chimera 39 (a2) outer surfaces within one icosahedral unit. They have a BeAn background, with the GDVII replacements outlined in white. (b) Surface contour of one icosahedral unit of BeAn (b1). The region including the VP3 GH loop and the gap is boxed in red. The corresponding boxed regions for chimeras 41 and 39 are enlarged in b2 and b3, respectively, with the program GRASP.

cluster B is located at VP2 puff B (21) (the nomenclature for the secondary structure elements is according to Luo et al. [20]. Figure 3a highlights the amino acid differences between BeAn and GDVII on the outer surface of one GDVII icosahedral asymmetric unit. Although the main chain structures are similar in the cluster B regions of all known TMEV structures, the side chains including an Arg have different orientations. In BeAn virus, the carboxyl group of Asp-2170 (the residues are designated by four numbers; the first indicates the viral protein, and the last three indicate the position from the N terminus) forms a hydrogen bond with the side chain of Arg-2172 and the side chain of Trp-1095. The latter is probably mediated by a water molecule. In DA virus, the carboxyl group of Asp-2170 forms a hydrogen bond with the side chain of Arg-2168. In both BeAn and DA viruses, the side chain of Asp-2170 is in approximately the same direction and the side chain of Arg-2172 points to the solvent toward VP1 in the northeastern direction. In GDVII virus, however, Arg-2172 is replaced by a Gln that forms a hydrogen bond with the side chain of Arg-2168. As a consequence, the side chain of Asp-2170 is also relocated, although Asp-2170 is the same amino acid residue for all three viruses. In addition, the side chain of Arg-2171 in GDVII virus replaces Ser-2171 in both BeAn and DA viruses and points to the solvent in the northwestern direction, about 90° to the side chain of Arg-2172 in both BeAn and DA viruses. Such a rearrangement leads to the relocation of two charges. Furthermore, variant residues between virus groups are distributed around a gap between VP1 and VP2 surface loops. These residues are 1060 to 1063, 1076 to 1086, 1093 to 1097, and 1109 from VP1 and 2169 to 2172 from VP2 (Fig. 3a and b). Variant residues 1076 and 1077, 1079, 1084, and 1093 to 1096 from VP1 are not exposed on the capsid surface. However, these unexposed residues could influence the conformation of the exposed surface residues through direct or long-distance interactions. This gap has a similar shape and charge distribution in BeAn and DA viruses, but it is quite different in GDVII virus. It is interesting to note that although Glu-1060 is a conserved amino acid and the main chain structures are similar in these two groups of viruses, the side chain orientation of Glu-1060 is dramatically different in these two groups of viruses. In the less virulent and persistent parental BeAn and DA viruses, the side chain of Glu-1060 points toward the gap in a direction perpendicular to the radial axis. In the highly virulent and nonpersistent parental GDVII virus, the side chain of Glu-1060 points to the solvent in a direction roughly parallel to the radial axis. A similar situation was observed for

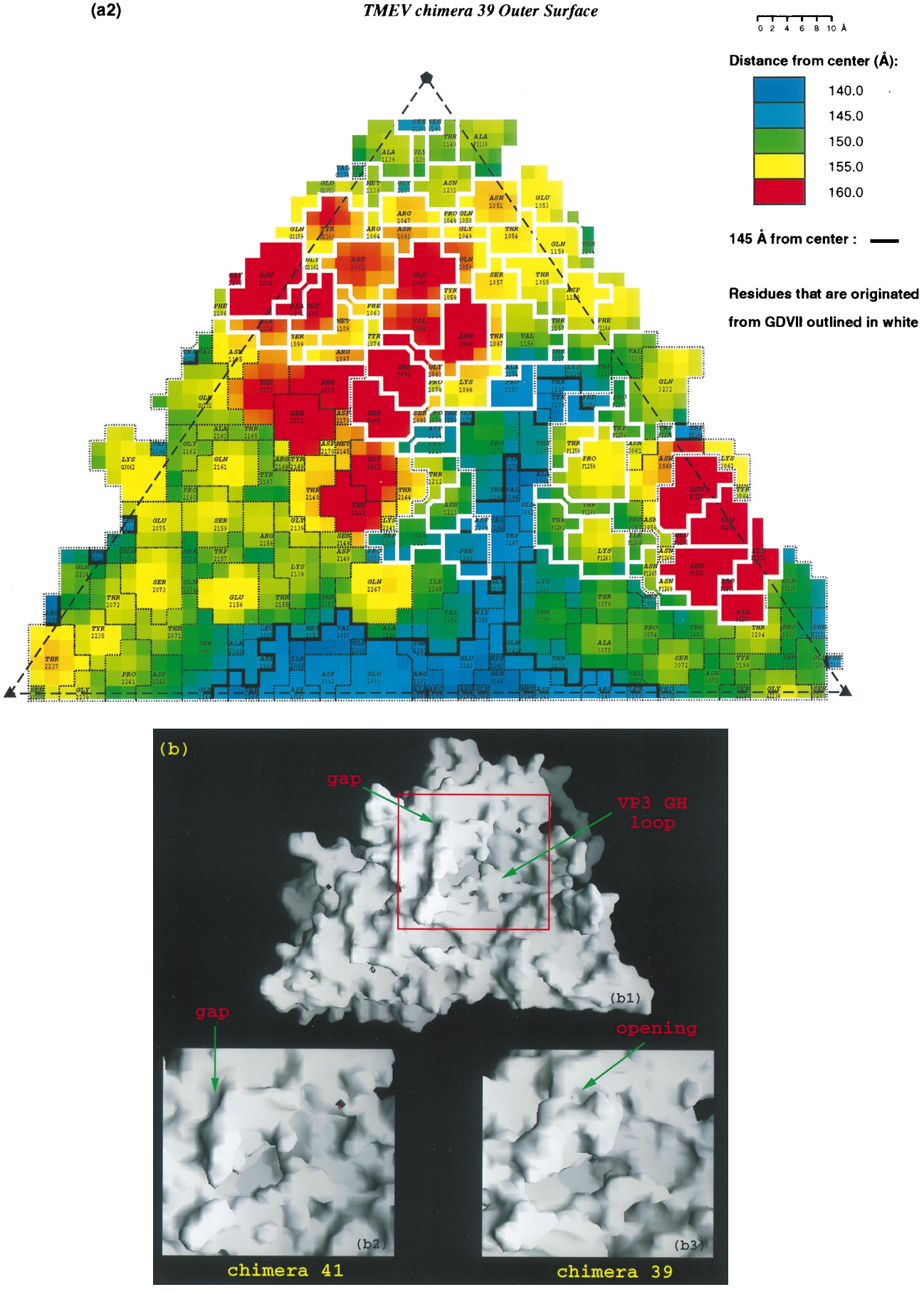

FIG. 4—*Continued.*

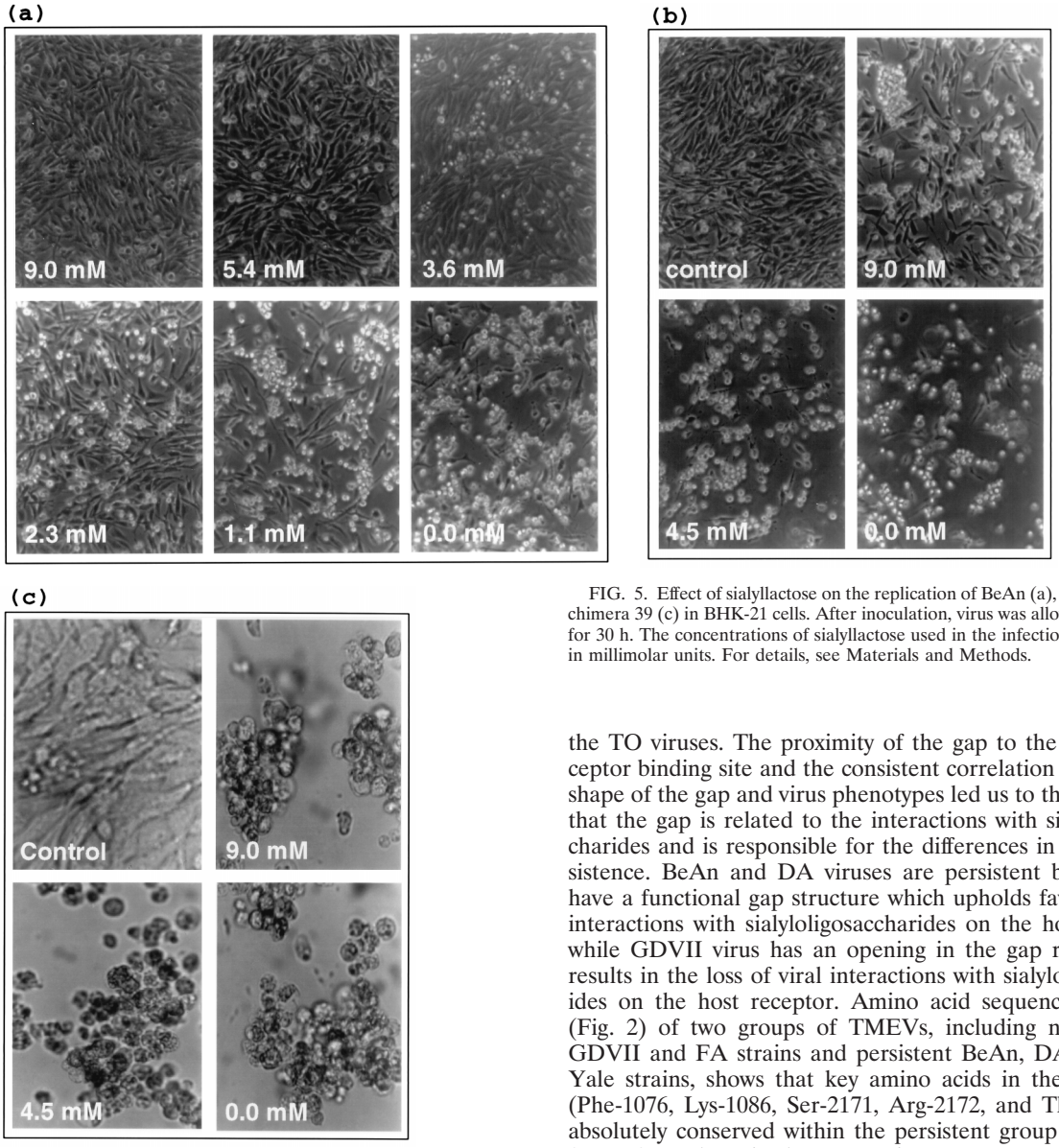

FIG. 5. Effect of sialyllactose on the replication of BeAn (a), GDVII (b), and chimera 39 (c) in BHK-21 cells. After inoculation, virus was allowed to replicate for 30 h. The concentrations of sialyllactose used in the infections are indicated in millimolar units. For details, see Materials and Methods.

the side chain of residue 1086. In BeAn and DA viruses, 1086 is a Lys and its side chain points into the gap, forming a salt bridge with the Glu-1060 side chain. In GDVII virus, Lys-1086 is replaced by an Arg and its side chain points away from the gap and to the solvent in the radial direction; as a result, there is an opening between residues Glu-1060 and Arg-1086.

Consequently, the gaps formed by residues from both VP1 and VP2 were shaped differently in these two phenotypically different groups of viruses (Fig. 3c). The virus surface contour revealed by GRASP (Fig. 3c) shows clearly that the gap is right next to the putative receptor binding site near the VP3 GH loop (22). Early studies by Fotiadis et al. (9) on the attachment of GDVII and BeAn viruses to intact BHK-21 cells showed that these two groups of viruses share a common receptor but bind to the receptor differently. GDVII and BeAn viruses competed with each other for the receptor, but virus attachment was inhibited by neuraminidase desialylation only for BeAn virus and not for GDVII virus. This result suggests that sialyloligosaccharides may be part of the cellular receptor for the TO viruses. The proximity of the gap to the putative receptor binding site and the consistent correlation between the shape of the gap and virus phenotypes led us to the hypothesis that the gap is related to the interactions with sialyloligosaccharides and is responsible for the differences in TMEV persistence. BeAn and DA viruses are persistent because they have a functional gap structure which upholds favorable viral interactions with sialyloligosaccharides on the host receptor, while GDVII virus has an opening in the gap region which results in the loss of viral interactions with sialyloligosaccharides on the host receptor. Amino acid sequence alignment (Fig. 2) of two groups of TMEVs, including neurovirulent GDVII and FA strains and persistent BeAn, DA, TO4, and Yale strains, shows that key amino acids in the gap region (Phe-1076, Lys-1086, Ser-2171, Arg-2172, and Thr-2173) are absolutely conserved within the persistent group but are different from those in the nonpersistent group.

Structural differences in TMEV chimeras. Much effort went into constructing chimeras between the highly virulent GDVII virus and the less virulent, persistent BeAn and DA viruses in an attempt to define finer regions in the capsid proteins which are the determinants for TMEV persistence. For instance, chimeras 39 and 41 have the same genomic construction except for the length of the GDVII replacement (Fig. 1). Chimera 39 has a longer GDVII replacement (corresponding to residues 1032 to 1276 in VP1) than chimera 41 (corresponding to residues 1170 to 1276 in VP1). Based on the predicted model constructed by merging the corresponding coordinates from GDVII and BeAn, followed by MODELLER refinement, the chimera 41 capsid retains most of the outer surface features of BeAn virus, such as the gap, because the surface residues originating from GDVII are not located near the gap (Fig. 4a1 and b). In contrast, chimera 39 contains more GDVII residues; therefore, the surface features have lost the characteristics of BeAn virus (Fig. 4a2 and b). The shape of the gap in the chimera correlates well with either the persistence of chimera 41 or the nonpersistence of chimera 39 (2), as in the parental

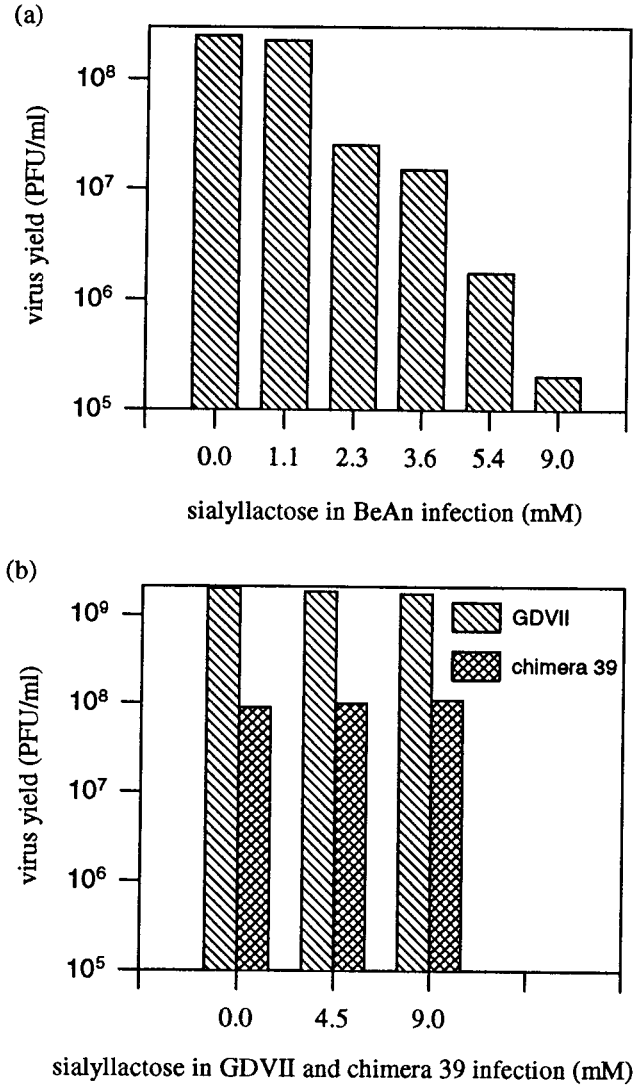

FIG. 6. Growth of BeAn (a) and GDVII and chimera 39 (b) in BHK-21 cells in the presence of sialyllactose. Cells were infected with BeAn, GDVII, or chimera 39 in the presence of different concentrations of sialyllactose. Virus titers were determined by a plaque assay with BHK-21 cells. For details, see Materials and Methods.

viruses. This pair of chimeric viruses suggests that residues 1032 to 1169 in VP1 and some residues in VP2 of BeAn bear a major or at least a partial determinant for viral persistence. On the other hand, chimeras 29 and 38 have a GDVII background with BeAn replacements at residues 1171 to 1276 in VP1 and 2001 to 2237 in VP2, respectively (Fig. 1). The predicted models of chimeras 29 and 38 do not exhibit BeAn characteristics in the gap region, a result consistent with the fact that both chimeras 29 and 38 were not persistent in the CNS during mouse infection (2). Apparently, the interaction between residues from both VP1 and VP2 and not residues from VP1 or VP2 alone defines a specific conformation, such as in the gap region, which determines viral persistence. The same is observed for DA-GDVII chimeric viruses. In a persistent hybrid between DA and GDVII viruses, pGD5′ (15), VP1 and residues 2153 to 2267 of VP2 are the same as those in DA virus, resulting in a DA-like gap region (data not shown).

However, an exceptional case was found with a persistent chimera, pGD1B, which contains a GDVII background with a DA replacement only at residues 2001 to 2152 (15). This chimera was assembled with an *Nco*I restriction site that lies between the sequences encoding VP2 puff A and puff B (Fig. 2 and 3a). The critical location of the *Nco*I site was revealed by Jarousse et al. (15), who found that pGD1B persisted only when DA residue 2141 on the tip of puff A was a Lys but not when it was an Asn, as in chimera pTMR4. Since the predicted model of pGD1B showed no surface feature similar to those of the other persistent parental and chimeric viruses, the reason why pGD1B persists is not clear. Based on the predicted models of pGD1B and pTMR4, residue 2141 is adjacent to the fragment from residues 2169 to 2173, which is part of the proposed structural determinant, the gap, for viral persistence, and is next to residue Thr-2142, which is absolutely conserved within the persistent group but not in the nonpersistent group (Fig. 2). Residue 2141 is also across the gap from residue 1101, which controls the ability of DA virus to persist in the CNS. DA virus became nonpersistent when VP1 loop II residue 1101 was changed from Thr to Ile (37–39). Compared to the sequences of GDVII virus (ANGA) and BeAn virus (VNGA), the sequence of DA virus (-TT) has a shorter VP1 loop II and two amino acid sequence variations. It was also reported that when DA Thr-1101 was replaced with an Ala or when two amino acids were inserted after Thr, the ability of the mutant viruses to persist was either reduced or abolished, whereas assembly of the complete VP1 loop II structure of GDVII in the DA background restored persistence (36). Therefore, like the residues in the 1101 region, residue 2141 may be a modulator which defines the conformation and charge distribution of the gap region to control viral persistence.

Role of sialyloligosaccharides in BeAn replication. To test whether sialyloligosaccharides affect the replication of TMEVs in BHK-21 cells, virus infection in the presence of different concentrations of sialyllactose was carried out for BeAn, GDVII, and chimera 39. BeAn was shown to infect and induce CPE in BHK-21 cells in the presence of 0.0, 1.1, and 2.3 mM sialyllactose, while 5.4 and 9.0 mM sialyllactose prevented CPE (Fig. 5a). In the presence of 3.6 mM sialyllactose, plaques were observed. The virus yield was determined by a plaque assay with BHK-21 cells (Fig. 6a). The virus yield was reduced by roughly 10- to 100-fold at each increment of sialyllactose concentration, with a 10^5- to 10^6-fold reduction at 9.0 mM. The

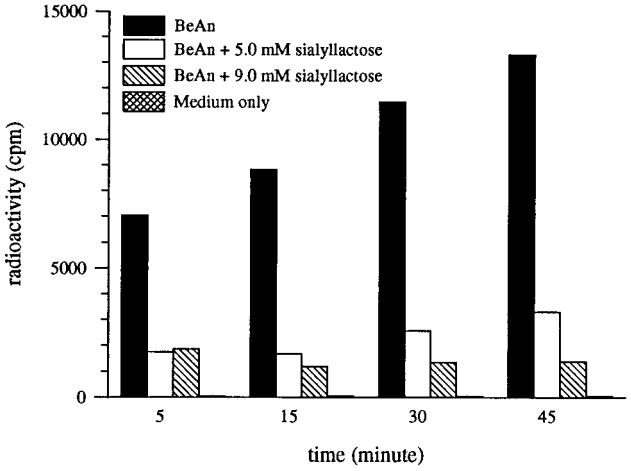

FIG. 7. Time course of ^{35}S-labeled BeAn virus binding to BHK-21 cell monolayers in the presence of 0.0, 5.0, and 9.0 mM sialyllactose. For details, see Materials and Methods.

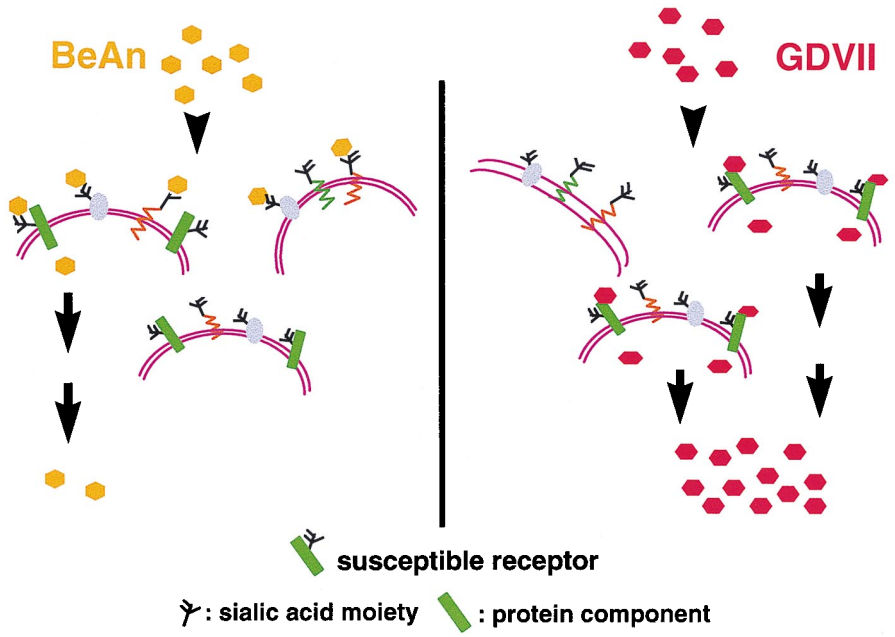

FIG. 8. Proposed model for TMEV persistence.

different cellular changes caused by BeAn infection in the presence of sialyllactose at various doses indicated that sialyllactose reduced BeAn replication in BHK-21 cells and that inhibition was dose dependent. In contrast, CPE was observed with all the GDVII and chimera 39 infections in the presence of 0.0, 4.5, and 9.0 mM sialyllactose (Fig. 5b and c). There was no difference in virus yield from GDVII or chimera 39 infections (Fig. 6b). High concentrations (10 and 50 mM) of lactose did not affect either BeAn or GDVII infections in BHK-21 cells (data not shown). Based on the chemical properties of sialyllactose and the results of Fotiadis et al. (9), it is likely that sialyllactose inhibits BeAn virus infection by blocking cellular attachment. A virus binding assay with ^{35}S-labeled BeAn virus did indeed show that 5.0 and 9.0 mM sialyllactose reduced BeAn virus binding to BHK-21 cells by about 75 and 90%, respectively (Fig. 7). Nonradiolabeled BeAn virus was shown to inhibit the binding of radiolabeled BeAn virus. To eliminate the possibility that sialyllactose affected BeAn virus binding by altering the host cell surface, ^{35}S-labeled BeAn virus binding was measured with BHK-21 cells pretreated with 9.0 mM sialyllactose followed by three washes with cold PBS. There was no detectable change in the level of binding of ^{35}S-labeled BeAn virus to BHK-21 cells with or without sialyllactose pretreatment (data not shown). This result implies that sialyllactose binds to BeAn virus and inhibits infection by blocking binding to the cellular receptor. All of these results support our hypothesis that the different viral surface features of BeAn and GDVII, such as the proposed gap, correlate with differences in host receptor binding and viral persistence. The results demonstrate that BeAn virus binds to the host cell in a different way than GDVII virus and, therefore, presents a different phenotype.

The relationship of sialic acid to infection with BeAn virus was first implied in the sensitivity of BeAn binding to BHK-21 cells treated with neuraminidase (9) and is now demonstrated by the work presented in this report. It was shown that 3′-sialyllactose, three sugar molecules of common oligosaccharides borne on the surface of most mammalian cells at certain concentrations, could prevent CPE in BHK-21 cells infected with BeAn virus but not GDVII virus or chimera 39. The virus yield from BHK-21 cells was gradually reduced with increasing 3′-sialyllactose concentration in cells infected with BeAn but, again, not in cells infected with GDVII or chimera 39. A binding assay with ^{35}S-radiolabeled BeAn virus further demonstrated that 3′-sialyllactose inhibited BeAn infection by blocking virus binding to the host cell. These results provide evidence for sialic acid as the BHK-21 cell receptor fragment only for BeAn virus and not for GDVII virus.

The ability to bind to sialyloligosaccharides has also been implicated in the phenotypic differences of other viruses, such as polyomavirus. In a study of murine polyomavirus tumor induction in mice, it was found that a single amino acid in the VP1 protein (Glu-91) could influence the profile of tumor growth and was shown to be involved in receptor recognition (10). This Glu-91 is part of the attachment site for the second sialic acid on a polyomavirus branched-chain oligosaccharide receptor fragment revealed by X-ray crystallography (33). BeAn and DA form small plaques on BHK-21 cells and cause mild damage to neurons in mouse brain, whereas GDVII forms large plaques and causes severe damage. It has been demonstrated that the restrained viral replication of persistent strains is not due to viral RNA synthesis (4). Hence, the ability of persistent strains to bind sialyloligosaccharides could be one of the factors that slows down the spread of newly synthesized virions and allows the virus to persist. In order to persist, the virus must cause only limited damage to the CNS because the survival of critical numbers of infected cells is a basic requirement for viral persistence. A model for TMEV persistence is proposed in Fig. 8. For productive infection, both BeAn and GDVII have to bind to the susceptible receptor on the host cell. The interaction of BeAn and its susceptible receptor involves both a protein component and sialic acid on the receptor. The ability of BeAn to bind to sialic acid on a nonsusceptible receptor traps BeAn and slows down the spread of newly synthesized BeAn to other uninfected cells. GDVII does not bind to sialic acid, and the interaction of GDVII with its sus-

ceptible receptor seems to involve only the protein component on the receptor. The selective binding of GDVII to the cell surface gives GDVII a much higher rate of spread to uninfected cells and makes GDVII more productive than BeAn. Although no clear elucidation for sialyloligosaccharide involvement in TMEV persistence is available, our results indicate some connections among viral surface features, sialyloligosaccharide binding, and viral persistence. Establishing the relationship between the ability to bind sialyloligosaccharides and different TMEV phenotypes needs further characterization with other TMEV strains, such as DA, as well as phenotypically different recombinant viruses.

Nonviable chimeric genomes. Some chimeric genomes constructed between GDVII and BeAn viruses were not viable. This fact may be related to the capsid assembly around the fivefold vertices, which showed different patterns of stabilizing interactions. In the initial structure of BeAn virus, a piece of electron density was found on the fivefold axis, but no ligand for this density could be identified. In an improved electron density map of the BeAn structure, the side chain density of Lys-3011 in VP3 was close to the extra density. Thus, the positively charged side chains of Lys-3011 may serve as ligands for this density, which may be a negatively charged molecule, such as borate in the buffer used for crystallization, on the fivefold axis. Only cations and not negatively charged molecules on the fivefold axis have been reported in other picornavirus structures. In GDVII virus, residue 3011 is an Asp, which could not be a ligand for a negatively charged molecule, and no extra density was found on the fivefold axis. GDVII appears to be able to stabilize the virion at the fivefold axis without ions. In foot-and-mouth disease virus, five Cys-3007 side chains of VP3 form a ring structure around the fivefold axis containing disordered disulfide bridges made by four of the five residues (1). In GDVII virus, five symmetrically related Ser-1180 residues in VP1 form a circular hydrogen bond network around the fivefold axis. Therefore, it is possible that GDVII employs a different mechanism to stabilize its virion at the fivefold axis. The amino terminus of VP3 extends beneath VP1 at the fivefold position, where the sequence-variable region cluster A is located. The amino-terminal end of VP3 forms a β-cylinder around the fivefold axis connecting the five protomers corresponding to the 14S pentameric assembly unit. The five parallel β-strands in the β-cylinder have a right-handed twist. This β-cylinder was also observed in Mengo virus (20). The fivefold axis has been postulated to be the site at which the myristylated N termini of VP4 are exposed during disassembly. Binding of the fivefold cation in human rhinoviruses has been associated with virion stability, which is affected by pH, antiviral compounds (WIN), and drug-resistant mutations (12, 17).

Chimeras 34, 35, and 36 all have a hybrid version of capsid protein at the fivefold vertices. They contain a BeAn VP1 background and a GDVII VP3 amino terminus. The altered interaction between VP1 and VP3 subunits at the fivefold vertices in chimeras 34, 35, and 36 would change the stability of protomer and pentamer structures in these chimeras. Viable virions were not observed when these constructs were used to transfect BHK-21 cells (2). Any chimera that imposes a defect in any step of viral capsid assembly and conformational change in the putative receptor binding site may be a nonviable or noninfectious construct. Chimera 37 has a BeAn background with a GDVII substitution of residues 2001 to 2136 in VP2. The energy for a chimera 37 protomer (VP1, VP2, and VP3) calculated by X-PLOR would be very high if there were no adjustment of side chains at the interfaces of subunits. There would be collisions between subunits VP1 and VP2, such as residues Tyr-2036 to Cys-1247, Arg-2168 to Trp-1095, and Phe-2176 to Leu-1117. There has to be conformational rearrangement in order to assemble a stable chimera 37 protomer, which may result in the failure of proper pentamer or protomer assembly or conformational changes at the host receptor binding sites.

ACKNOWLEDGMENTS

We thank Carl X. Zhang and Lily Yang for technical assistance.

This work was supported by grants from NIH to M.L. (NS23349) and to H.L.L. (NS21913).

REFERENCES

1. **Acharya, R., E. Fry, D. Stuart, G. Fox, D. Rowlands, and F. Brown.** 1989. The three-dimensional structure of foot-and-mouth disease virus at 2.9 Å resolution. Nature **337:**709–716.
2. **Adami, C., A. E. Pritchard, T. Knaut, M. Luo, and H. L. Lipton.** Unpublished data.
3. **Arnold, E., M. Luo, G. Vriend, M. G. Rossmann, A. C. Palmenberg, G. D. Parks, M. J. H. Nicklin, and E. Wimmer.** 1987. Implications of the picornavirus capsid structure for polyprotein processing. Proc. Natl. Acad. Sci. USA **84:**21–25.
4. **Aubert, C., and M. Brahic.** 1995. Early infection of the central nervous system by the GDVII and DA strains of Theiler's virus. J. Virol. **69:**3197–3200.
5. **Brünger, A. T.** 1992. X-PLOR manual, Version 3.1. Yale University, New Haven, Conn.
6. **Calenoff, M. A., K. S. Faaberg, and H. L. Lipton.** 1990. Genomic regions of neurovirulence and attenuation in Theiler's murine encephalomyelitis virus. Proc. Natl. Acad. Sci. USA **87:**978–982.
7. **Chapman, M. S.** 1993. Mapping the surface properties of macromolecules. Protein Sci. **2:**459–469.
8. **Daniels, J. B., A. M. Pappenheimen, and S. Richardson.** 1952. Observations on encephalomyelitis of mice (DA strain). J. Exp. Med. **96:**22–24.
9. **Fotiadis, C., D. R. Kilpatrick, and H. L. Lipton.** 1991. Comparison of the binding characteristics to BHK-21 cells of viruses representing the two Theiler's virus neurovirulence groups. Virology **182:**365–370.
10. **Freund, R., R. L. Garcea, R. Sahli, and T. L. Benjamin.** 1991. A single amino acid substitution in polyomavirus VP1 correlates with plaque size and hemagglutination behavior. J. Virol. **65:**350–355.
11. **Fu, J., S. Stein, L. Rosenstein, T. Bodwell, M. Routbort, B. L. Semler, and R. P. Roos.** 1990. Neurovirulence determinants of genetically engineered Theiler's viruses. Proc. Natl. Acad. Sci. USA **87:**4125–4129.
12. **Giranda, V. L., B. A. Heinz, M. A. Oliveira, I. Minor, K. H. Kim, P. R. Kolatkar, M. G. Rossmann, and R. R. Rueckert.** 1992. Acid-induced structural changes in human rhinovirus 14: possible role in uncoating. Proc. Natl. Acad. Sci. USA **89:**10213–10221.
13. **Grant, R. A., D. J. Filman, R. S. Fujinami, J. P. Icenogle, and J. M. Hogle.** 1992. Three-dimensional structure of Theiler's virus. Proc. Natl. Acad. Sci. USA **89:**2061–2065.
14. **Hogle, J. M., M. Chow, and D. J. Filman.** 1985. Three-dimensional structure of poliovirus at 2.9 Å resolution. Science **229:**1358–1365.
15. **Jarousse, N., R. A. Grant, J. M. Hogle, L. Zhang, A. Senkowski, R. P. Roos, T. Michiels, M. Brahic, and A. McAllister.** 1994. A single amino acid change determines persistence of a chimeric Theiler's virus. J. Virol. **68:**3364–3368.
16. **Jones, T. A.** 1985. Diffraction methods for biological macromolecules. Interactive computer graphics: FRODO. Methods Enzymol. **115:**157–171.
17. **Kim, K. H., P. Willingmann, Z. X. Gong, M. J. Kremer, M. S. Chapman, I. Minor, M. A. Oliveira, M. G. Rossmann, K. Anderies, G. D. Diana, et al.** 1993. A comparison of the anti-rhinoviral drug binding pocket in HRV14 and HRV1A. J. Mol. Biol. **230:**206–227.
18. **Lipton, H. L.** 1975. Theiler's virus infection in mice: an unusual biphasic disease process leading to demyelination. Infect. Immun. **11:**1147–1155.
19. **Lipton, H. L.** 1980. Persistent Theiler's murine encephalomyelitis virus infection in mice depends on plaque size. J. Gen. Virol. **46:**169–177.
20. **Luo, M., G. Vriend, G. Kamer, I. Minor, E. Arnold, M. G. Rossmann, U. Boege, D. G. Scraba, G. M. Duke, and A. C. Palmenberg.** 1987. The atomic structure of Mengo virus at 3.0 Å resolution. Science **235:**182–191.
21. **Luo, M., C. He, K. S. Toth, C. X. Zhang, and H. L. Lipton.** 1992. Three-dimensional structure of Theiler murine encephalomyelitis virus (BeAn strain). Proc. Natl. Acad. Sci. USA **89:**2409–2413.
22. **Luo, M., K. S. Toth, L. Zhou, A. Pritchard, and H. L. Lipton.** 1996. The structure of a highly virulent Theiler's murine encephalomyelitis virus (GDVII) and implications for determinants of viral persistence. Virology **220:**246–250.
23. **McAllister, A., F. Tangy, C. Aubert, and M. Brahic.** 1990. Genetic mapping of the ability of Theiler's virus to persist and demyelinate. J. Virol. **64:**4252–4257.
24. **Michiels, T., N. Jarousse, and M. Brahic.** 1995. Analysis of the leader and capsid coding regions of persistent and neurovirulent strains of Theiler's virus. Virology **214:**550–558.

25. **Nicholls, A., K. Sharp, and B. Honig.** 1991. Protein folding and association—insights from the interfacial and thermodynamic properties of hydrocarbons. Proteins Struct. Genet. **4:**281–296.
26. **Ohara, Y., S. Stein, J. Fu, L. Stillman, L. Klaman, and R. P. Roos.** 1988. Molecular cloning and sequence determination of DA strain of Theiler's murine encephalomyelitis viruses. Virology **164:**245–255.
27. **Pevear, D. C., M. Calenoff, E. Rozhou, and H. L. Lipton.** 1987. Analysis of the complete nucleotide sequence of the picornavirus Theiler's murine encephalomyelitis virus indicates that it is closely related to cardioviruses. J. Virol. **61:**1507–1516.
28. **Pevear, D. C., J. Borkowski, M. Calenoff, C. K. Oh, B. Ostrowski, and H. L. Lipton.** 1988. Insights into Theiler's virus neurovirulence based on a genomic comparison of the neurovirulent GDVII and less virulent BeAn strains. Virology **165:**1–12.
29. **Rossmann, M. G., E. Arnold, J. W. Erickson, E. A. Frankenberger, J. P. Griffith, H. J. Hecht, J. E. Johnson, G. Kamer, M. Luo, A. G. Mosser, R. R. Rueckert, B. Sherry, and G. Vriend.** 1985. Structure of a human common cold virus and functional relationship to other picornaviruses. Nature **317:** 145–153.
30. **Rossmann, M. G., and A. C. Palmenberg.** 1988. Conservation of the putative receptor attachment site in picornaviruses. Virology **164:**373–382.
31. **Šali, A., and T. L. Blundell.** 1990. Definition of general topological equivalence in protein structures: a procedure involving comparison of properties and relationships through simulated annealing and dynamic programming. J. Mol. Biol. **212:**403–428.
32. **Šali, A.** 1992. A protein structure modeling program.
33. **Stehle, T., and S. C. Harrison.** 1996. Crystal structures of murine polyomavirus in complex with straight-chain and branched-chain sialyloligosaccharide receptor fragments. Structure **4:**183–194.
34. **Theiler, M.** 1934. Spontaneous encephalomyelitis of mice: a new virus disease. Science **80:**122–123.
35. **Toth, K. S., C. X. Zhang, H. L. Lipton, and M. Luo.** 1993. Crystallization and preliminary X-ray diffraction studies of Theiler's virus (GDVII strain). J. Mol. Biol. **231:**1126–1129.
36. **Wada, Y., M. L. Pierce, and R. S. Fujinami.** 1993. The loop II of VP-1 is one of the major determinants for Theiler's virus induced disease, abstr. A37. *In* Abstracts of the 12th Annual Meeting of the American Society for Virology.
37. **Wada, Y., M. L. Pierce, and R. S. Fujinami.** 1994. Importance of amino acid 101 within capsid protein VP1 for modulation of Theiler's virus-induced disease. J. Virol. **68:**1219–1223.
38. **Zurbriggen, A., and R. S. Fujinami.** 1989. A neutralization-resistant Theiler's virus variant produces an altered disease pattern in the mouse central nervous system. J. Virol. **63:**1505–1513.
39. **Zurbriggen, A., C. Thomas, M. Tamada, R. P. Roos, and R. S. Fujinami.** 1991. Direct evidence of a role for amino acid 101 of VP-1 in central nervous system disease in Theiler's murine encephalomyelitis virus infection. J. Virol. **65:**1929–1937.